SUPPLEMENTARY MATERIAL

Tables (6), Figures and Legends (11), Footnotes (3)

Genetic dissection of an amygdala microcircuit that gates conditioned fear

Wulf Haubensak[1], Prabhat Kunwar[1*], Haijiang Cai[1*], Stephane Ciocchi[3*], Nicholas Wall[4], Ravikumar Ponnusamy[5], Jonathan Biag[6], Hong-Wei Dong[6], Karl Deisseroth[7], Edward M. Callaway[4], Michael S. Fanselow[5], Andreas Lüthi[3] and David J. Anderson[1,2,8]

[1]Division of Biology 216-76

[2]Howard Hughes Medical Institute

California Institute of Technology

Pasadena, CA USA 91125

[3]Friedrich Miescher Institute for Biomedical Research

4058 Basel, Switzerland

[4]Systems Neurobiology Laboratory

The Salk Institute for Biological Studies

La Jolla, CA 92037

[5]Department of Psychology and the Brain Research Institute

[6]Laboratory for Neuroimaging

University of California, Los Angeles

Los Angeles, CA 90095

[7]Department of Bioengineering

Stanford University

Stanford, CA 94305

Supplementary Table 1. Overlap of neuronal marker and PKCδ expression in CEl.

	Marker/PKCδ	PKCδ/Marker
Gad65	87.4±4.7	50.3±12.6
CRH	1.2±1.0	16.9±15.2
Dyn	1.9±1.2	4.5±2.9
Enk	42.8±7.4	71.3±6.8
OxtR	65.3±9.7	81.1±1.9

Percent cells expressing marker or PKCδ ±SEM (n=3-5).

Supplementary Table 2. Membrane properties of the three types of CEl neurons.

	n	%	R_{input} (MΩ)	V_m rest (mV)	Delay (ms)	AP1 Amp (mV)	Half width (ms)	Threshold (mV)	Rise time (ms)
Late-firing	21	55	391±45	-61±2	223±21	65.4±2.0	3.6±1.3	-35.0±1.2	0.8±0.1
Regular spiking	14	37	414±59	-56±2	60±8	65.4±4.1	2.5±0.3	-41.7±1.3	0.8±0.1
Low-threshold bursting	3	8	492±40	-51±1	25±10	67.7±11.7	1.5±0.1	-41.0±1.1	0.7±0.02
***P* value**			0.77	0.20	<0.0001	0.99	0.49	0.0009	0.94

* Delay is measured from the start of current injection to the start of the first action potential. AP1 Amp, half width, threshold, and rise time are analysed from the first action potential evoked by current injection. *P*-value compares late-firing and regular spiking neurons, 2-tailed t-test.

Supplementary Table 3. Electrophysiological type of PKCδ$^+$ and PKCδ$^-$ cells in CEl.

	n	Type	*n*	Incidence
PKCδ$^+$	14	Late-firing	12	86%
		Regular spiking	2	14%
		Low threshold	0	0%
PKCδ$^-$	12	Late-firing	5	42%
		Regular spiking	6	50%
		Low threshold	1	8%

Retrospective assignment of electrophysiological types to PKCδ$^+$ or PKCδ$^-$ neurons after neurobiotin filling and PKCδ IFL (see Fig. 1m, n).

Supplementary Table 4. Relation of PKCδ expression and electrophysiological type.

	Late-firing	**Other**	**Total**
CEl total	21	17	38
PKCδ$^+$	49	8	57

The electrophysiological subtype assignment of the PKCδ$^+$ population (Table S3) was confirmed by recording from prospectively identified PKCδ$^+$ neurons using GluClα-CFP native fluorescence as a marker. 49 out of 57 PKCδ$^+$ cells were late-firing neurons, while 8 out of 57 PKCδ$^+$ cells were regular spiking neurons. No low-threshold bursting neurons were represented in the PKCδ$^+$ population. Fisher's exact test with significant interaction of PKCδ expression and firing properties (P = 0.0016).

Supplementary Table 5. Tone test data, blocked by infection rate.

Block	Infection (%)		BL Freezing (%)		CS Freezing (%)		post-CS Freezing (%)	
	Control	Expt	Control	Expt	Control	Expt	Control	Expt
1	0.1±0.1	2.8±0.7	1.3±0.8	8.1±4.0 (n. s.)	70.0±7.4	61.1±11.6 (n. s.)	31.4±10.8	51.1±8.8 (n. s.)
2	2.9±0.6	6.9±0.4	5.0±1.8	4.4±0.8 (n. s.)	83.5±4.3	53.0±6.0 (n. s.)	36.8±7.1	19.2±6.3 (n. s.)
3	6.7±0.5	8.6±0.2	2.5±1.2	1.4±0.8 (n. s.)	21.9±3.9	47.7±10.5 (n. s.)	4.2±1.2	35.6±15.4 (n. s.)
4	10.4±0.7	10.2±0.2	2.3±0.8	5.8±3.1 (n. s.)	42.7±10.9	69.4±12.2 (n. s.)	21.4±6.8	45.3±11.1 (n. s.)
5	13.6±0.2	12.1±0.3	4.1±3.2	2.5±0.8 (n. s.)	44.9±13.9	53.5±12.0 (n. s.)	18.1±6.3	33.6±11.9 (n. s.)
6	17.2±0.5	14.9±0.6	5.2±3.1	2.8±1.0 (n. s.)	58.6±12.1	55.6±13.3 (n. s.)	33.4±12.0	24.4±9.8 (n. s.)
7	27.7±2.1	19.6±0.7	3.7±1.7	8.9±4.0 (n. s.)	67.2±8.0	66.5±11.7 (n. s.)	32.2±6.6	51.9±13.8 (n. s.)
8	35.6±0.9	24.6±1.2	1.7±0.7	1.9±0.8 (n. s.)	44.6±10.8	64.3±12.7 (n. s.)	30.6±8.1	36.5±14.6 (n. s.)
9	40.0±0.8	40.6±3.5	5.8±2.2	2.6±1.5 (n. s.)	49.4±10.4	91.1±4.7 ($P < 0.05$)	19.2±6.0	75.3±8.4 ($P < 0.001$)

Data are mean ± SEM. A Randomized Block ANOVA[1] with 6 experimental and control subjects assigned to each of 9 blocks based on infection rate (total $n = 108$) revealed a significant block x group interaction for CS ($F_{(8, 90)} = 2.298$, $P < 0.05$; with a significant linear component indicating that the difference between groups tended to increase with infection rate: $F_{(1,90)} = 22.98$, $P < 0.0001$) and post-CS ($F_{(8, 90)} = 2.459$, $P < 0.05$; linear component: $F_{(1, 90)} = 8.85$, $P < 0.006$), but not BL periods ($F_{(8,90)} = 1.41$, $P = 0.205$). *P* is from post-hoc Bonferroni t-test values. n.s., not significant. For graphic representation of the data see Fig. S5. "Expt," experimental group (PKCδ::GluClα−ires-Cre transgenic mice injected with AAV::GluClβ virus and treated with IVM). The control group contains both wild-type animals injected with the GluClβ virus, and transgenic (PKCδ::GluClα) animals injected with the GluClα virus; these controls were not significantly different from each other (Supplementary Figure 4) and were pooled for this analysis. All control animals in this comparison were treated with IVM. In some experiments, animals expressing GluClαβ, but not treated with IVM were included (see also Figures S6 and S7). The number of mice in this additional control group was too small to include in the overall ANOVA shown above. However, among those mice in this group with an infection rate within the range of the animals in block 9 (37.3±2.5%; $n = 3$), the freezing rates for the different conditions were similar to those in the control group of block 9 (BL = 3.7±1.0%; CS = 57.2±9.6%; post-CS = 18.3±2.2%). This –IVM group was also significantly different from the IVM-treated experimental group, when animals with a bilateral AAV infection rate above the median for the population were compared using non-parametric statistics (Fig. S7).

Supplementary Table 6. Injection coordinates.

	Bregma	Lateral	Ventral
CEl	-1.4	2.9	4.8
CEm	-1.0	2.4	4.6
PAG	-4.8	0.5	3.0

Values in mm.

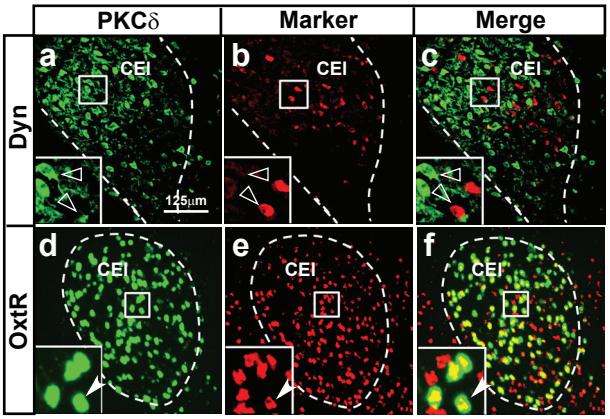

Supplementary Fig.1. Phenotypic characterization of CEl PKCδ$^+$ neurons. dIFL (**a-c**) and dFISH (**d-f**) reveals that PKCδ$^+$ neurons do not express dynorphin (**a-c**), but express oxytocin receptor (**d-f**). Filled and open arrowheads, doubly vs. singly labeled cells, respectively. Scale bar for all panels.

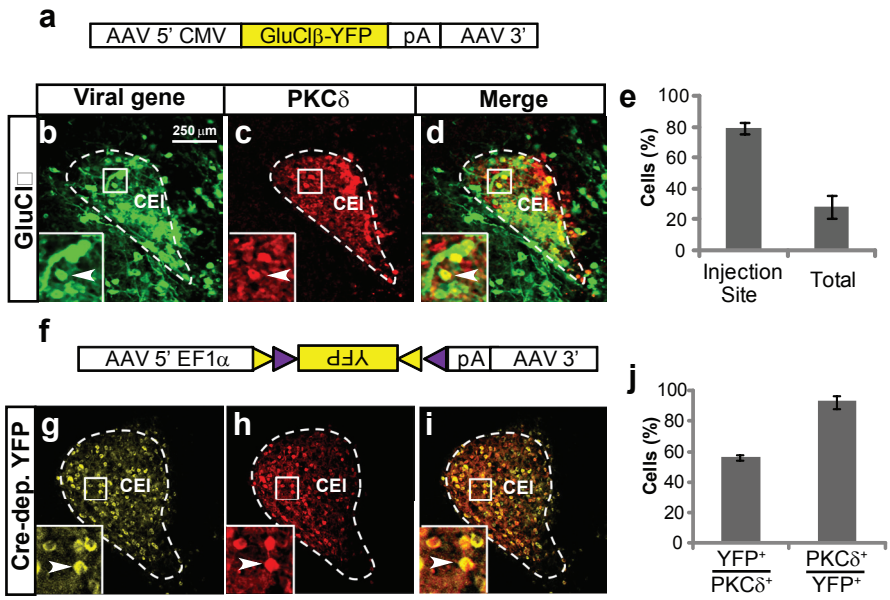

Supplementary Fig. 2. Viral targeting and Cre-dependent expression in CEl PKCδ⁺ cells. a-e, Expression of AAV2::GluClβ-subunit (**a**) after stereotaxic intra-amygdala injections of virus in CEl . **b-d**, GluClβ-YFP and PKCδ expression were detected by anti-GFP and anti-PKCδ antibody staining. Wild-type mice were injected to permit immunofluorescent detection of GluClß-YFP with anti-GFP antibodies, without cross-reaction of the antibody to the transgene-encoded GluClα-CFP. **e**, Quantification of the fraction of GFP immunoreactive PKCδ⁺ cells in (**b-d**), (*left*) within 0.1 mm surrounding the injection site, and (right) within CEl as a whole ($n = 4$). **f-j**, Region and cell type specific expression of a Cre-dependent YFP reporter gene in CEl PKCδ⁺ neurons by intra-amygdala injection of Cre-dependent AAV (**f**) into PKCδ::GluClα−iCre mice. **g-i**, YFP native fluorescence (**g**) and anti-PKCδ antibody staining (**h**). **j**, Quantification of data in (**g-i**). *Left*, Efficiency of YFP-delivery ($n = 6$) among CEl PKCδ⁺ cells. *Right*, Specificity of Cre-dependent YFP expression for PKCδ+ cells ($n = 6$). Scale bar for **b-d**, **g-i**.

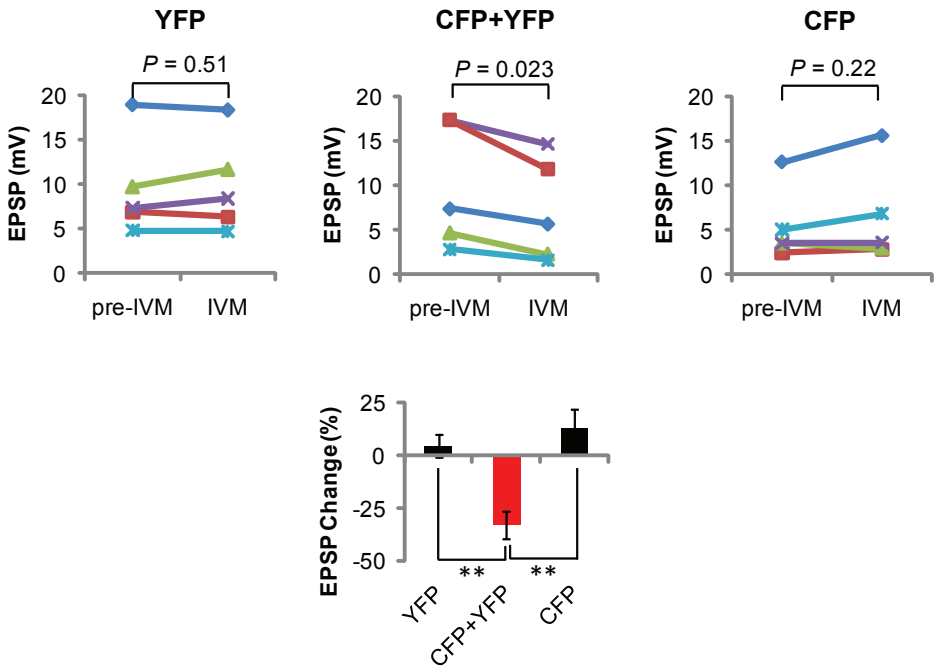

Supplementary Fig. 3. EPSPs are significantly decreased in neurons that express both GluClα-CFP and GluClβ-YFP after IVM treatment. EPSPs of individual cells (*top*) and average (*bottom*) in response to IVM (n = 5; One-way ANOVA ($F_{(2, 12)}$ = 11.36, P = 0.0017) with post-hoc Bonferroni t-test (** $P < 0.01$).

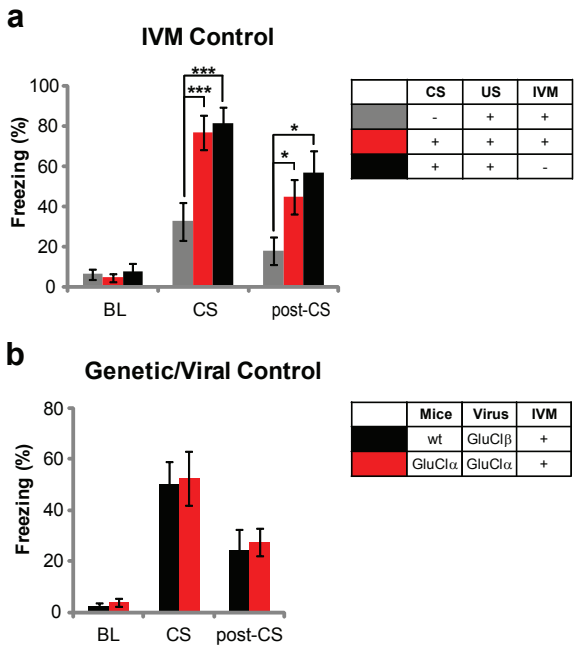

Supplementary Figure 4. IVM, genetic and viral controls of pharmacogenetic silencing in vivo. a, IVM does not affect fear conditioning. Wild-type mice injected with IVM (n = 10) showed significant freezing during the CS exposure and post-CS when compared to US-only controls (n = 9), and were indistinguishable from vehicle injected animals (n = 8). One-way ANOVA during BL ($F_{(2, 24)}$ = 0.287, P = 0.753), CS ($F_{(2, 24)}$ = 9.091, P = 0.001) and post-CS ($F_{(2,24)}$ = 4.901, P = 0.016) periods with Fisher's LSD (*** $P < 0.01$, * $P < 0.05$). **b**, Freezing in genetic and viral controls is comparable. "Genetic control" is AAV2::GluClβ-injected wild-type animals (n = 7; infection rate 37±1.4 PKCδ$^+$ cells); "viral control" is PKCδ::GluClα-iCre transgenic mice injected with AAV2::GluClα rather than with GluClβ virus (n = 8; infection rate 36.3±1.3 PKCδ$^+$ cells). T-tests during BL (P = 0.808), CS (P = 0.520) and post-CS (P = 0.955) periods. Based on these results, data from these two types of control animals were pooled in subsequent experiments. BL, baseline freezing prior to first CS presentation; CS, conditioned stimulus.

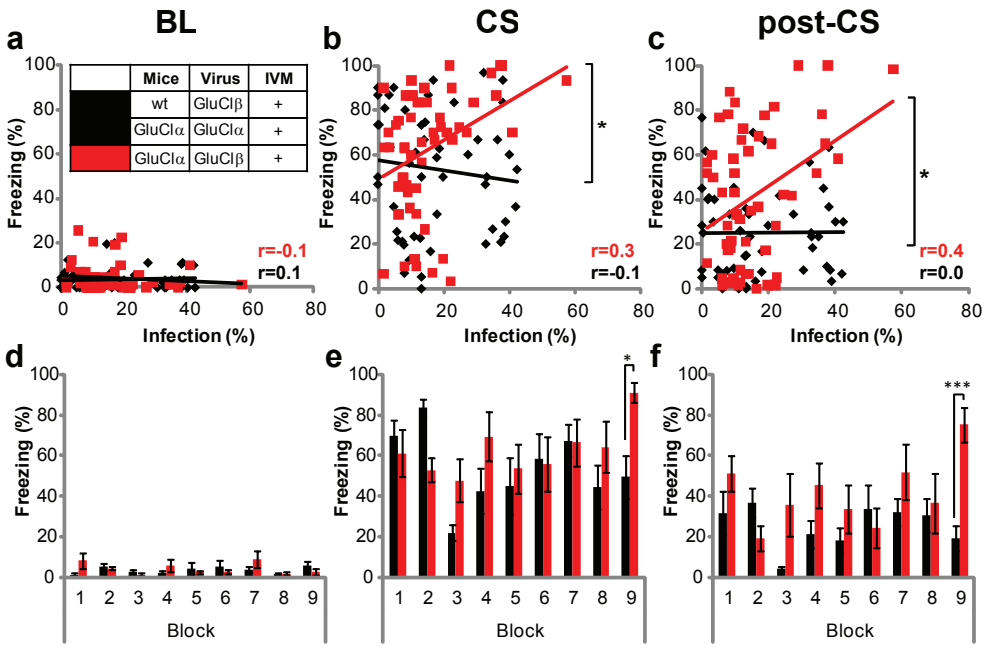

Supplementary Fig. 5. **Behavioral effect of silencing PKCδ$^+$ neurons in CEl is positively correlated with infection. a-c**, Scatter plots of the experimental data reveal a significant correlation of behavioral phenotype with frequency of infection of PKCδ$^+$ neurons in experimental (red line; AAV2::GluClβ-injected PKCδ::GluClα-iCre transgenic mice) but not in genetic and viral control mice (black line; pooled, see Fig. S4b). Infection rate was estimated for each animal by immunofluorescence labeling for PKCδ and GluClβ-YFP fluorescence (see Methods and Figure S10). Statistics for pooled control groups: $r_{BL} = 0.071$, $P_{BL} = 0.608$, $R^2_{BL} = 0.005$, $r_{CS} = -.011$, $P_{CS} = 0.412$, $R^2_{CS} = 0.013$, $r_{ITI} = 0.009$, $P_{ITI} = 0.949$, $R^2_{ITI}=0.000$; $n = 54$. Statistics for experimental mice: $r_{BL} = -0.125$, $P_{BL} = 0.639$, $R^2_{BL} = 0.004$, $r_{CS} = 0.360$, $P_{CS} = 0.0075$, $R^2_{ITI} = 0.1294$, $r_{ITI} = 0.375$, $P_{ITI} = 0.005$, $R^2_{ITI} = 0.141$; $n = 54$; with significant differences in slopes (* $P < 0.05$). No significant differences between experimental and control groups were observed during training (not shown). **d-f**, Graphic representation of the blocked ANOVA of the experimental data described in Table S5.

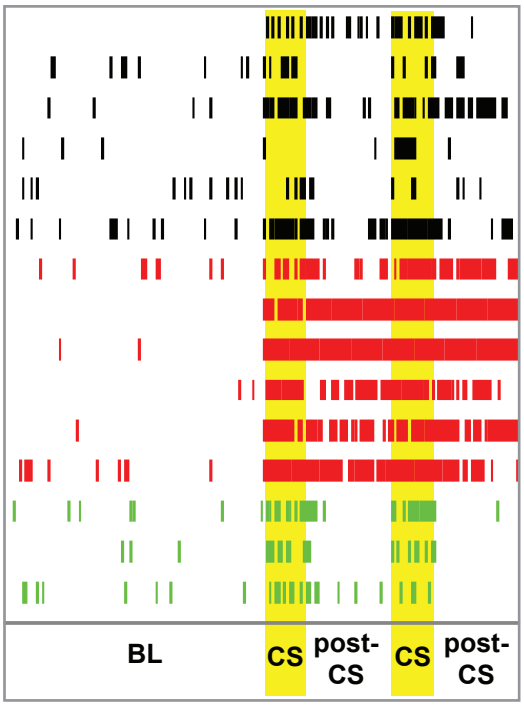

	Mice	Virus	IVM
	wt	GluClβ	+
	GluClβ	GluClα	+
	GluClα	GluClβ	+
	GluClα	GluClβ	-

Supplementary Fig. 6. Freezing episodes plotted in 2 sec bins during the tone test session of IVM-treated single-subunit (GluClα− or GluClβ− expressing) control (n = 6, black) and IVM-treated experimental (GluClαβ -expressing) mice (n = 6, red) derived from block 9 in Tables I, S5, Fig. S5d-f. The data for GluClαβ-expressing control mice not treated with IVM (n = 3, green) were taken from animals with equal infection rates to those in block 9 (35.5 ± 2.5%). The comparison is for illustrative purposes only. See Fig. S7 for a statistical analysis of differences between these 3 groups. Note the persistence of freezing into the post-CS period in experimental animals (red rasters).

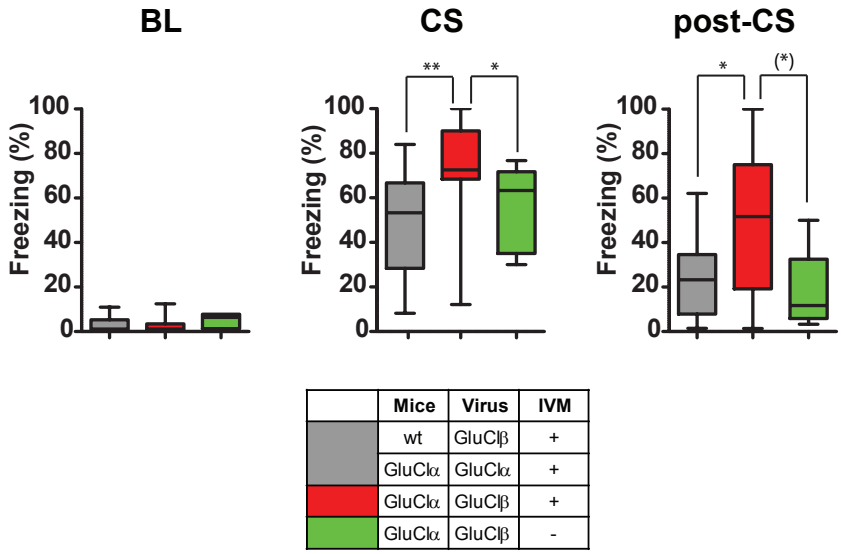

	Mice	Virus	IVM
	wt	GluClβ	+
	GluClα	GluClα	+
	GluClα	GluClβ	+
	GluClα	GluClβ	-

Supplementary Fig. 7. Behavioral effect of silencing PKCδ$^+$ neurons in animals with bilateral infection. The data represent animals exhibiting AAV infection in CEl in both hemispheres, at a level above the median infection rate of the population, and are pooled from multiple experiments (Fig. S5). Box plots show medians and interquartile ranges for the 3 groups described in the table. The single-subunit IVM-treated control mice (wild-type injected with GluClβ virus, or transgenic ("GluClα") mice injected with GluClα virus) were not significantly different from each other (Supplementary Figure 4b) and were pooled for this analysis (n = 21; gray bar). This control group, the experimental group (GluClαβ +IVM, n = 17; red bars), and an additional control group expressing GluClαβ but not treated with IVM (n = 6; green bars), were analyzed using non-parametric statistics, because the data were not normally distributed and the sample sizes were not equal. BL (baseline) period: one-way Kruskal-Wallis ANOVA (H = 1.94, P = 0.38). CS period: one-way Kruskal-Wallis ANOVA (H = 11.14, P = 0.0038); * P < 0.05, ** P < 0.01; one-tailed Mann-Whitney post-hoc test corrected for multiple comparisons. post-CS period: one-way Kruskal-Wallis ANOVA (H = 6.73, P = 0.0346); * P < 0.05, one-tailed Mann-Whitney post-hoc test with Bonferroni correction for multiple comparisons. (*) indicates significant to P < 0.03 without correction for multiple comparisons, but not significant (P < 0.06) when corrected.

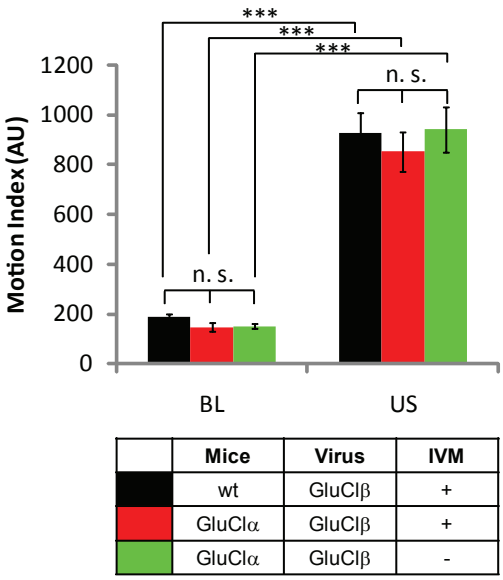

Supplementary Fig. 8. Suppression of CEl PKCδ^{+} neuronal activity does not change locomotor activity or US sensitivity. Control (black, $n = 9$, average infection rate 53.9 ± 9.0 %) and experimental mice 12 h after a single dose of 10 mg/kg IVM (red, $n = 13$, average infection rate 49.9 ± 6.9 %), or injected with vehicle (green, $n = 13$, average infection rate 52.0 ± 6.8 %), show similar levels of baseline locomotor activity during 20 min in the training context prior presentation of the first CS (*left*) and during exposure to the first US (right; One-way ANOVA ($F_{(2, 32)} = 0.46$, $P = 0.64$)), which induced a significant comparable burst in locomotor activity in all groups (Two-way ANOVA ($F_{(1, 32)}$=283.85, $P < 0.0001$) with post-hoc Bonferroni t-test (*** $P < 0.001$). The absence of any substantial differences in US reactivity makes it unlikely that the observed effect on freezing (Fig. 3f) is merely consequence of increased US sensitivity[2]. Values are mean ± SEM.

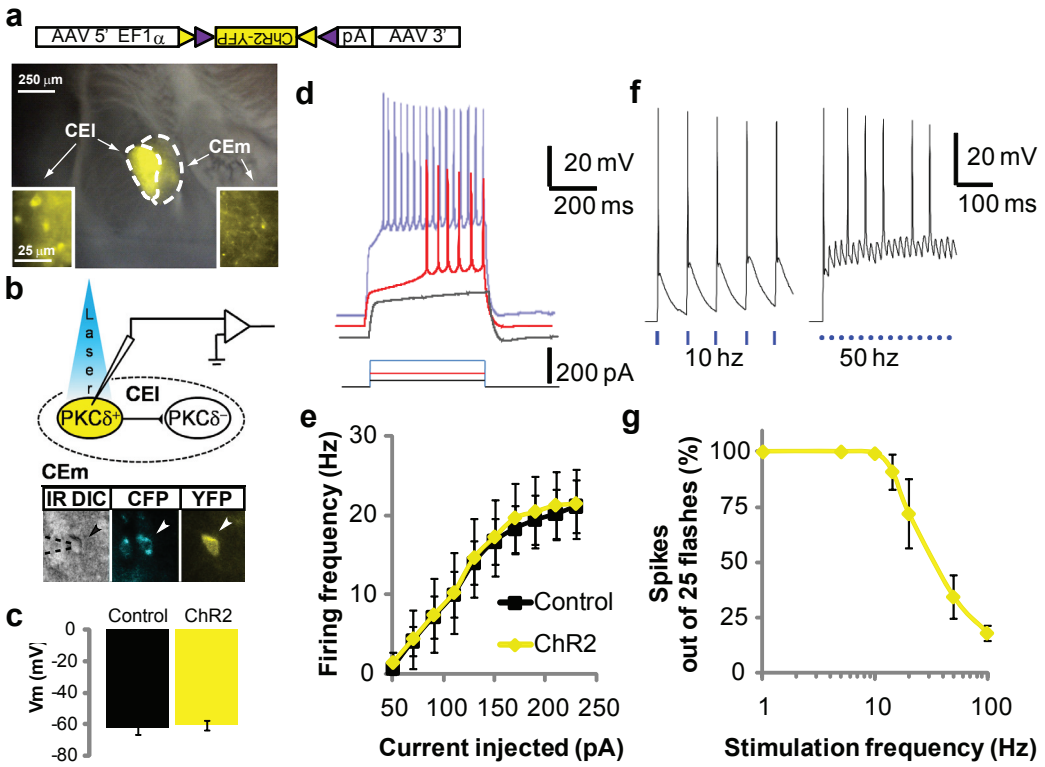

Supplementary Fig. 9. Physiological properties are unchanged in PKCδ$^+$ cells that express ChR2. a, Selective expression of ChR2 in CEl PKCδ$^+$ neurons after intra amygdala injection of Cre-dependent AAV5::ChR2-YFP into PKCPKC δ::GluClα-CFP-iCre transgenic mice. Note CEm projecting axonal fiber tracts of ChR2-YFP-expressing CEl PKCδ$^+$ neurons (arrows). **b**, Single cell expressing both CFP (PKCδ$^+$) and YFP (ChR2$^+$). **c**, Resting membrane potentials of ChR2 expressing PKCδ$^+$ neurons (n = 5 cells), were identical to that of PKCδ$^+$ neurons not expressing ChR2 (n = 7 cells). **d**, Spiking properties of CEl PKCδ$^+$ neurons in response to injections of weak (black), medium (red) or strong (blue) depolarizing currents, in whole-cell current-clamp recordings. **e**, Comparison of experiments such as those in (**d**) performed in ChR2-YFP$^+$ (n = 5 cells) vs. ChR2-YFP$^-$ (n = 7 cells) PKCδ$^+$ neurons. The spiking rate as a function of depolarizing current injection is not affected by expression of ChR2. **f**, Light evoked spiking of ChR2 expressing PKCδ$^+$ neurons triggered by 2 ms laser pulses (blue bars) at the indicated frequencies. **g**, Percentage of successful spikes evoked by 25 2 ms laser pulses is stable up to 12 Hz, but decreases with higher frequencies (n = 5 cells).

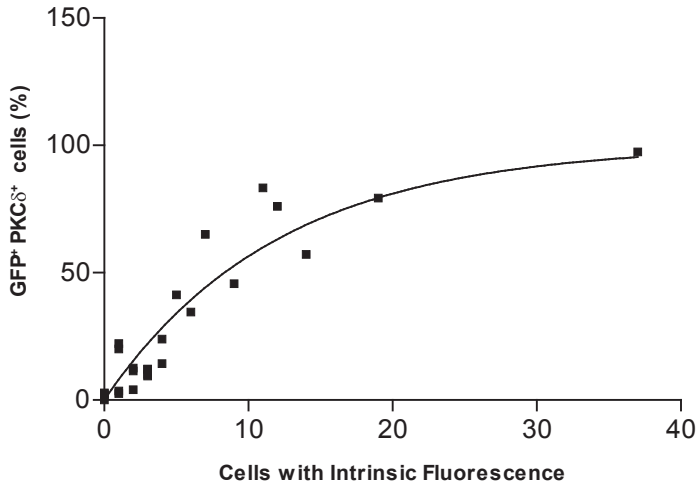

Supplementary Fig. 10. Relationship between YFP intrinsic fluorescence and GFP-immunoreactivity in CEl PKCδ$^+$ neurons following infection with AAV::GluClβ-YFP. The data illustrate the standard curve used to estimate the fraction of PKCδ$^+$ cells immunoreactive for GFP per CEl section based on the number of CFP/YFP$^+$ cells detected by intrinsic fluorescence. The curve was generated using data from GluClα or GluClβ virus injections into wt animals and each data point was collected from the same section. See Methods for further details.

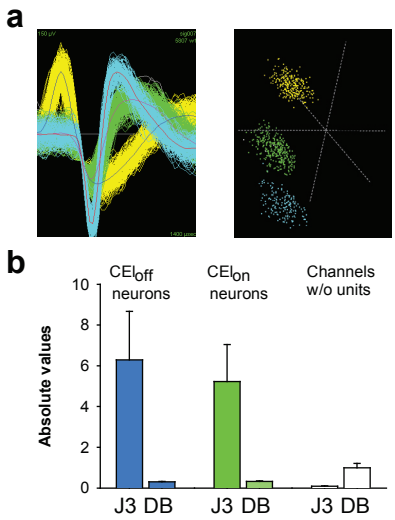

Supplementary Fig. 11. Isolation of single unit recordings. **a**, *Top left*, Superimposed waveforms recorded from three different units. *Top right*, Spikes originating from individual units were sorted using 3D-principal component analysis. **b**, Quantitative J3 and Davies Bouldin validity index (DB) statistics calculated for CEloff and CElon neurons. Controls values were obtained using two clusters defined from the centered cloud of points from channels in which no units could be detected. High values for the J3 and low values for the DB are indicative of good single unit isolation.

SUPPLEMENTARY FOOTNOTES

Supplementary Footnote 1

Several technical factors likely contribute to the variability in behavioral experiments in which PKCδ$^+$ neurons are silenced using the combination of PKCδ::GluClα transgene- + AAV-driven expression of GluClβ. In addition to the variability inherent in behavioral experiments, the two most important technical variables appear to be the accuracy of the injections, and the quality/titer of the virus preparation. As described in the main text, statistically significant differences between experimental (AAV2::GluClβ → PKCδ::GluClα transgenic/IVM) and single subunit-expressing control (AAV2::GluClα → PKCδ::GluClα transgenic/IVM, or AAV2::GluClβ → wild-type/IVM) groups were seen only among animals that had a high level and/or efficient bilateral expression of the virus in CEl (Table I, Fig. S5, S7 and Table S5). We have also experienced variability according to the particular preparation of AAV used. Initial experiments were performed using a very high-titer (~10^{13}/ml) preparation of AAV2[CMV::GluClβ] made commercially by Virapur, Inc. This virus preparation, which yielded the strongest effects in our experiments, was also successfully used in conjunction with an AAV2[CMV::GluClα] virus, prepared in parallel, to silence neurons in the striatum in an IVM-dependent manner[3], and also yielded strong IVM-dependent electrophysiological silencing of spontaneous spiking in PKCδ$^+$ neurons in thalamic slices, when injected into PKCδ::GluClα-ires-Cre transgenic mice (C. Xiao, W.H., W. Lerchner, H. Lester and D.J.A., unpublished data). Subsequent commercial preparations of this virus were less effective. Preparations of AAV GluClβ virus made using serotypes AAV5 or AAV8 did not measurably improve results. In general, it has been more difficult to generate high-titer AAV for the CMV::GluClβ construct, than for many other viral constructs we have produced. Based on our experience, the following technical variables are likely important in achieving significantly increased freezing upon silencing PKCδ$^+$ neurons in vivo:

1. Strong (above median levels), bilateral expression of AAV::GluClβ in CEl
2. Balanced expression of GluClα and GluClβ
3. Minimal spread of AAV::GluClβ virus into non-PKCδ::GluClα-expressing regions of the amygdala.

In addition to these technical sources of variation, biological factors may contribute to variability in the results as well. For example, "ceiling effects" may limit the ability to detect significantly increased freezing caused by silencing PKCδ$^+$ neurons during the period of CS-exposure, especially in well-trained animals. This is suggested by our observation that the magnitude of the difference between experimental and control groups was greater during the post-CS period, when freezing levels in control animals are returning towards baseline, than during CS-exposure (Fig. S6). This may reflect the possibility that activation of PKCδ$^+$ neurons plays a particularly important role in extinguishing freezing during the CS-off period, so that silencing these neurons during this interval has a relatively greater effect on freezing. Finally, given the reciprocal inhibition between PKCδ$^+$/CEl$_{off}$ and PKCδ$^-$/CEl$_{on}$ units, and the potentially symmetrical inhibition of CEm output neurons by these competing CEl units (but see Supplementary Footnote 3), it is possible that silencing PKCδ$^+$ neurons can, under some conditions, cause opposing influences on CEm activity that cancel each other out. Nevertheless,

our in vivo recordings indicate that silencing PKCδ$^+$ neurons caused only a slight and statistically non-significant increase in CEl$_{on}$ tonic activity, while CEm tonic activity was significantly increased. However the impact of silencing PKCδ$^+$ neurons on CEl$_{on}$ and CEm unit activity during CS exposure remains to be examined.

Supplementary Footnote 2

There are several differences between the effects of muscimol injections into CEl (Ciocchi et al., submitted), and the effects of IVM/GluCl-mediated silencing of PKCδ$^+$ neurons reported here. Injection of muscimol into CEl in untrained animals caused an increase in baseline (unconditional) freezing (Ciocchi et al.), while specific silencing of PKCδ$^+$ neurons did not cause any such increase. Furthermore, injection of muscimol into CEl 10 minutes before training strongly attenuated fear conditioning, while silencing of PKCδ$^+$ neurons throughout both the training and testing period caused an increase in CS-evoked freezing.

The difference in the effects of the two types of experimental manipulations on unconditional freezing may be explained by differences in their timing, cellular specificity and/or efficiency. Muscimol iontophoresis is performed acutely (10 minutes prior to testing); in contrast PKCδ:GluCl-expressing animals were tested 24 hrs after IVM administration. Since IVM at the concentration used reaches functional levels in the brain in ~12 hrs after administration[3], PKCδ$^+$ neurons in our experiments have been tonically suppressed in animals examined for baseline freezing; by contrast, muscimol is injected 30 min to 1 hr before testing, and produces an acute inhibition of CEl. Adaptation to tonic inhibition by IVM may explain the lack of an effect on unconditional freezing. In addition, and most importantly, muscimol injection targets all neurons within CEl, while IVM specifically inhibits only the PKCδ$^+$ subpopulation. Simultaneous inhibition of multiple CEl populations by muscimol may produce different behavioral effects than silencing of just the PKCδ$^+$ population. Finally, the efficiency of muscimol silencing is limited only by diffusion and the amount injected, since all neurons that express endogenous GABA receptors should be equally sensitive to the drug. By contrast, the efficiency of IVM silencing of PKCδ$^+$ neurons is limited by the fraction of those cells that express adequate levels of GluClα + GluClβ, which in turn depends on the efficiency of infection by AAV::GluClβ. Our data indicate that between 30-80% of PKCδ$^+$ neurons are typically infected by an AAV injection in CEl, depending on their distance from the injection site (Supplementary Figure S2e). Incomplete suppression of the PKCδ$^+$ population by IVM may explain why silencing this population after training increased the tonic activity of some individual CEm units, as detected electrophysiologically (Fig. 5m-n), but did not produce a measurable increase in baseline freezing. In summary, the difference between the effects of muscimol vs. selective silencing of PKCδ$^+$ neurons on baseline freezing may reflect differences in the relative cellular specificity (low vs. high), relative strength/efficiency (high vs. low), or time course (acute vs. chronic) of the two types of experimental manipulations.

Similar factors may explain why muscimol injection into CEl just prior to training inhibited fear conditioning, while silencing of PKCδ$^+$ neurons did not (but rather augmented CS-evoked freezing after training). The in vivo recordings of Ciocchi et al. suggest that after training, PKCδ$^-$ neurons are three times more likely to inhibit PKCδ$^+$ neurons, than vice-versa (see also Supplementary Footnote 3). If, during training, CEl$_{on}$ → CEl$_{off}$ inhibitory connections become

relatively stronger than CEl_{off} → CEl_{on} connections, then experimentally silencing $PKC\delta^{+}/CEl_{off}$ units would, if anything, only enhance the effect of training to strengthen the influence of CEl_{on} units. By contrast, since muscimol inhibits both $PKC\delta^{-}$ and the $PKC\delta^{+}$ populations, it would impair the development of dominance by the CEl_{on} population during training. In this way, the difference in the cellular specificity of the two manipulations could yield dramatically different behavioral effects. It is also possible that, due to its relative inefficiency (see above) partial silencing of the $PKC\delta^{+}$ population during training does not produce a sufficient overall reduction in inhibitory output from the CEl circuit to impair training, while muscimol silencing has a more highly penetrant effect.

Supplementary Footnote 3

If $PKC\delta^{+}$ neurons inhibit $PKC\delta^{-}$ neurons, and if both populations inhibit CEm output neurons (see also Ciocchi et al.), then why doesn't silencing $PKC\delta^{+}$ neurons *decrease* freezing (rather than increase it), via dis-inhibition of $PKC\delta^{-}/CEl_{on}$ neurons (thereby enhancing feed-forward inhibition by the latter onto CEm)? By the same token, why doesn't activation of $PKC\delta^{-}/CEl_{on}$ neurons by the CS reduce rather than enhance freezing? There are several possible explanations for this apparent paradox.

First, $PKC\delta^{+}$ and $PKC\delta^{-}$ neurons may inhibit a common population of CEm output neurons, but with different intrinsic strengths. If the $PKC\delta^{+}/CEl_{off}$ → CEm inhibitory connection is stronger than the $PKC\delta^{-}/CEl_{on}$ → CEm connection, then the net effect of the CS on CEm activity may be dominated by the change in the stronger inhibitory connection, and therefore a net increase in CEm activity would obtain. In the absence of molecular tools to specifically manipulate the $PKC\delta^{-}/CEl_{on}$ population, we cannot directly compare the relative strength of the $PKC\delta^{+}$ → CEm and $PKC\delta^{-}$ → CEm inhibitory connections. Nevertheless, even if the two connections are of similar strength, the fact that, after conditioning, the tonic activity of $PKC\delta^{+}/CEl_{off}$ neurons is greater than the tonic activity of $PKC\delta^{-}/CEl_{on}$ neurons (Ciocchi et al., Fig. 2) suggests that reducing the strong tonic inhibition by $PKC\delta^{+}$ neurons should have a greater influence on net CEm activity, than would enhancing the weak tonic inhibition by $PKC\delta^{-}$ neurons. Consistent with this idea, Ciocchi et al. observe that 85% of CEm units are excited by the CS in vivo, and we observe that silencing of $PKC\delta^{+}$ neurons leads to a net increase in CEm activity (Fig. 5m-n).

Second, it is not yet certain whether $PKC\delta^{+}$ and $PKC\delta^{-}$ CEl neurons synapse onto the same or different populations of CEm neurons. While we have shown that $PKC\delta^{+}/CEl_{off}$ neurons directly inhibit CEm neurons that project to the PAG, where freezing is controlled, there is no such direct evidence for the $PKC\delta^{-}/CEl_{on}$ population. There is evidence for connectional heterogeneity among CEm output neurons[4]. If $PKC\delta^{-}/CEl_{on}$ neurons do not directly inhibit CEm output neurons mediating freezing, then enhancing inhibition of their CEm target neurons would not interfere with freezing promoted by dis-inhibition of PAG-projecting CEm neurons controlled by the $PKC\delta^{+}$ population.

Third, because CEl_{on} ($PKC\delta^{-}$) neurons reciprocally inhibit $PKC\delta^{+}$ neurons, enhancing the activity of the former (whether via the CS, or via silencing of $PKC\delta^{+}$ neurons), will tend to further depress the activity of the latter population, leading to enhanced dis-inhibition of CEm.

Importantly, the CEl circuit appears inherently "biased" so that the response of the circuit to the CS is dominated by the activation of CEl_{on} neurons, as suggested by two observations:

1) As shown by Ciocchi et al., $CEl_{on} \rightarrow CEl_{off}$ inhibitory interactions are 3x more frequent than $CEl_{off} \rightarrow CEl_{on}$ (Ciocchi et al.) connections;

2) $PKC\delta^{-}$ (CEl_{on}) neurons are rapid-onset neurons, while $PKC\delta^{+}$ are delayed-onset firing neurons (this study); therefore activation of $PKC\delta^{-}$ neurons by the CS will occur prior to any activation of $PKC\delta^{+}$ neurons.

Thus, there is both a temporal and a connectional asymmetry in the response of the CEl inhibitory circuit to the CS, with CEl_{on} neurons both responding faster to the CS than CEl_{off} neurons, and inhibiting CEl_{off} neurons more strongly, than vice-versa. Given this asymmetry, and the fact that lateral interactions between CEl_{off} neurons and CEl_{on} neurons may be stronger than their feed-forward inhibition of CEm neurons, increasing the activity of CEl_{on} neurons may have a proportionately greater effect to depress the activity of $CEl_{off}/PKC\delta^{+}$ neurons, and thereby dis-inhibit CEm, than to further inhibit CEm directly.

In summary, given that activation of CElon neurons by the CS is associated with increased freezing, and given that the activity of CEloff ($PKC\delta^{+}$) neurons opposes the activity of CElon neurons, then experimental manipulations that reduce the activity of $PKC\delta^{+}$ neurons should enhance the response of CElon neurons to the CS, and thereby enhance freezing.

References

1 Edwards, A. L. *Experimental Design in Psychological Research*. 4th edn, 249-251 (Holt, Reinhard & Winston, 1972).

2 Wilensky, A. E., Schafe, G. E., Kristensen, M. P. & LeDoux, J. E. Rethinking the fear circuit: the central nucleus of the amygdala is required for the acquisition, consolidation, and expression of Pavlovian fear conditioning. *J Neurosci* **26**, 12387-12396, (2006).

3 Lerchner, W. *et al.* Reversible silencing of neuronal excitability in behaving mice by a genetically targeted, ivermectin-gated Cl- channel. *Neuron* **54**, 35-49, (2007).

4 LeDoux, J. E., Iwata, J., Cicchetti, P. & Reis, D. J. Different projections of the central amygdaloid nucleus mediate autonomic and behavioral correlates of conditioned fear. *J Neurosci* **8**, 2517-2529, (1988).